ISSN 1753-3562

June 2009 Volume 50 Number 3

Physics and Chemistry of Glasses

European Journal of Glass Science and Technology Part B

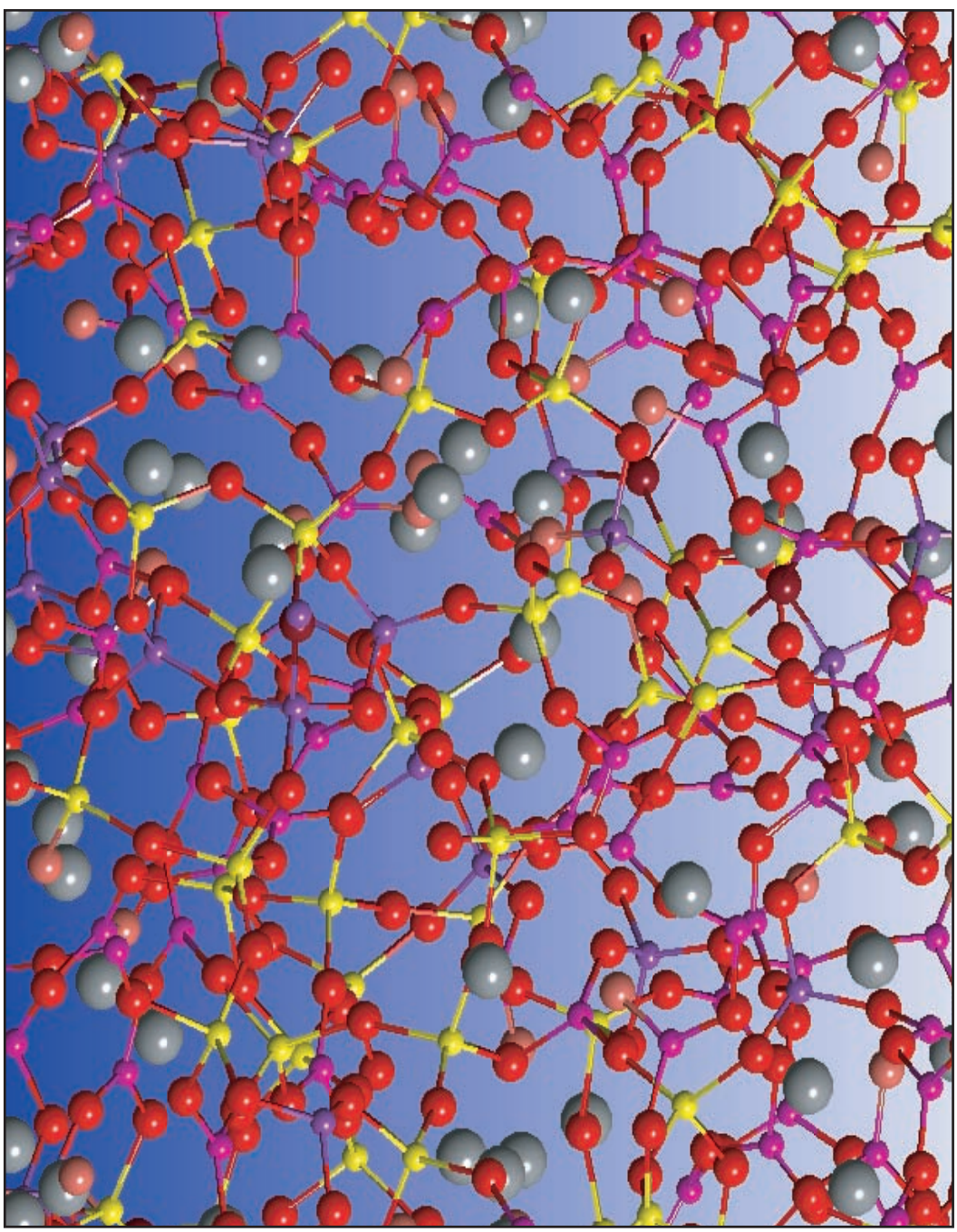

Volume 50 Number 3 June 2009

Physics and Chemistry of Glasses

European Journal of Glass Science and Technology B

The European Journal of Glass Science and Technology is a publishing partnership between the Deutsche Glastechnische Gesellschaft and the Society of Glass Technology. Manuscript submissions can be made through Editorial Manager, see the inside back cover for more details.

Society of Glass Technology
Unit 9, Twelve O'clock Court
21 Attercliffe Road
Sheffield S4 7WW, UK
Tel +44(0)114 263 4455
Fax +44(0)114 263 4411
E-mail info@sgt.org
Web http://www.sgt.org

The Society of Glass Technology is a registered charity no. 237438.

Advertising
Requests for display rates, space orders or editorial can be obtained from the above address.

Physics and Chemistry of Glasses: European Journal of Glass Science and Technology, Part B
ISSN 1753-3562 (Print)
ISSN 1750-6689 (Online)

The journal is published six times a year at the beginning of alternate months from February.

Electronic journals: peer reviewed papers can be viewed by subscribers through Ingenta Select
http://www.ingentaconnect.com

CONTENTS

PAPERS

PROCEEDINGS OF THE SIXTH CONF. ON BORATE GLASSES, CRYSTALS AND MELTS

Printed and bound by The Charlesworth Group, Wakefield, UK. Tel +44(0)1924 204830

Phys. Chem. Glasses: Eur. J. Glass Sci. Technol. B, February 2009, **50** (3), 137–143

An atomic scale comparison of the reaction of Bioglass® in two types of simulated body fluid

*V. FitzGerald, D. M. Pickup, D. Greenspan,[1] K. M. Wetherall, R. M. Moss, J. R. Jones[2] & R. J. Newport**

School of Physical Sciences, University of Kent, Canterbury, CT2 7NH, UK
[1] *Novamin Technology Inc., 13859 Progress Blvd., Alachua, FL 32615, USA*
[2] *Department of Materials, Imperial College London, London, SW7 2AZ, UK*

Manuscript received 11 April 2008
Revision received 8 December 2008
Manuscript accepted 8 December 2008

A class of melt quenched silicate glasses, containing calcium, phosphorus and alkali metals, and having the ability to promote bone regeneration and to fuse to living bone, is produced commercially as Bioglass. The changes in structure associated with reacting the bioglass with a body fluid simulant (a buffered Tris(hydroxymethyl)aminomethane growth medium solution or a blood plasma-like salt simulated body fluid) at 37°C have been studied using both high energy and grazing incidence x-ray diffraction. This has corroborated the generic conclusions of earlier studies based on the use of calcia–silica sol-gel glasses whilst highlighting the important differences associated with glass composition; the results also reveal the more subtle effects on reaction rates of the choice of body fluid simulant. The results also indicate the presence of tricalcium phosphate crystallites deposited onto the surface of the glass as a precursor to the growth of hydroxyapatite, and indicates that there is some preferred orientation to their growth.

1. Introduction

To allow people to remain active, and to contribute to society for longer, the need for new materials to replace and repair worn out and damaged tissues becomes ever more important. Bioglass is a bioactive material that has been shown to form a bond with bone when implanted into a bony defect.[1–3] The family of bioactive glasses are, in essence, calcium silicate glasses with additional alkali and alkaline-earth modifiers. The study of atomic-scale structure undertaken hitherto has largely been limited to indirect probes such as infrared spectroscopy, together with exploratory molecular dynamics, MD, simulation.[4,5] We have more recently published the first high energy x-ray and neutron diffraction (HEXRD, ND) data on this important material in the hope of providing more direct experimental insight into the glass structure; this has been supported using solid state NMR and RMC modelling.[6] In addition, a detailed structural study of the analogous, but compositionally simpler, calcium silicate sol-gel glass has been undertaken using HEXRD, ND and Raman spectroscopy.[7,8] Furthermore, the atomic scale structural changes associated with reacting the sol-gel analogues of this glass *in vitro* with simulated body fluid have been followed using *in situ*/time resolved HEXRD.[9]

A detailed quantitative knowledge of the structure of these bioactive glasses is a prerequisite for a full understanding of how changes in materials processing, composition, etc. affects *in vitro* reactivity and the resultant *in vivo* response of the body.

There is a significant difference between the experimentally measured x-ray and neutron diffraction patterns due to the differences in weighting factors associated with the fact that x-rays scatter from the distribution of electrons in the glass whereas neutrons scatter from the nuclei. This is shown graphically in Figure 1 for each distinct atom pair within the glass; the measured diffraction pattern will be a linear combination of these terms, weighted according to concentration within the glass. This figure demonstrates that x-ray diffraction data are to be preferred for studying the intermediate range order of oxide glasses, because the weighting factors of the Si…Si, Si…Ca and Ca…Ca correlations, which are strongly related to intermediate range order of these glasses, are relatively larger for x-rays than for neutrons. The figure also shows that neutron diffraction is better conditioned for obtaining data associated with O…O correlations (as well as for the provision of better resolved real space data *per se*, see below).

We here particularly seek to cast light upon the *in vivo* behaviour of the glass by undertaking an *in vitro* study of the reaction of the glass within simulated body fluid, SBF (a blood plasma-like salt solution[10]), or a buffered Tris(hydroxymethyl)aminomethane solution, TBS,[11] as a simulant of body fluid. HEXRD has been used to gather information on the changes to the glass structure, and grazing incidence x-ray diffraction, GIXRD, has been employed to provide additional, near-surface information on the material deposited during the reaction. In the latter experi-

* Corresponding author. Email r.j.newport@kent.ac.uk
This manuscript derives from the paper "A day in the life: calcium in Bioglass®" presented at the SGT's 2007 annual meeting in Derby.
Bioglass and Perioglass are a registered trade marks ®.

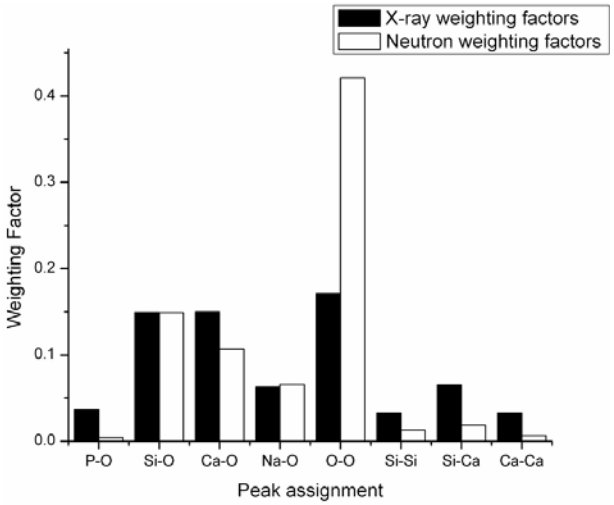

Figure 1. Pairwise scattering weighting factors associated with XRD, compared to those for a neutron diffraction experiment. (The total areas within the histogram have in both cases been normalised to unity)

ment, the angle of incidence is fixed at a low value (tending towards the critical angle for total external reflection, although still above it) in order to reduce the contribution to the diffraction pattern arising from the bulk glass itself.

The structure of the unreacted material has been studied using HEXRD, MAS-NMR and reverse Monte Carlo modelling.[6] The ^{29}Si NMR suggested that the host silica network primarily consists of chains and rings of Q^2 SiO_4 tetrahedra, with some degree of cross linking as represented by the presence of Q^3 units. The ^{31}P NMR indicated that phosphorus exists as isolated PO_4^{3-} anions in the structure, which could tend to remove sodium and calcium cations from a network modifying role in the silicate network.

The diffraction data showed a broad Ca–O pair correlation at ~2·05–2·90 Å, with a total coordination of ~5 and suggested a Na–O distance of 2·38 Å and a corresponding coordination of ~6. This coordination number was supported by the ^{23}Na NMR data, which revealed that the likely sodium environment is six-coordinate in pseudo-octahedral NaO_6 arrangement, although there is the possibility of the presence of five-coordinate Na^+ ions.

There was evidence of a non-homogeneous distribution of Na within the glass, which is important in the context of the relatively slow dissolution of the modified silica network. The data also provided evidence of Ca clustering, and implied the presence of CaO as the structural motif. This latter observation was of direct relevance to the understanding of the facile nature of Ca within such glasses which gives rise to its relatively rapid diffusion from the solid into solution (and therefore to its behaviour in terms of the material's overall bioactivity).

Table 1. Sample characterisation on the basis of x-ray fluorescence (using charge balancing to determine oxygen concentrations; the nominal batch silica content is 45 mol% and CaO:P_2O_5 molar ratio is 5, indicating some loss of P) and helium pycnometry

	45S5 (Bioglass)
Density / g cm^{-3} (±0·002)	2·708
Derived density / atoms Å^{-3}	0·07761
Composition / mol%	
CaO	26·9
SiO_2	46·1
P_2O_5	2·6
Na_2O	24·4
Derived at% (±0·003)	
Ca	0·101
Si	0·161
P	0·004
Na	0·083
O	0·651

2. Theory and experimental method

2.1. Sample preparation

The samples for HEXRD and GIXRD were supplied by Novamin Technology, Inc. in granular form and as disks respectively. The composition and density values for the samples are reported in Table 1. Composition analysis was performed using a Bruker S4 x-ray fluorescence instrument, and density measurements were based on helium pycnometry performed using a Quantachrome multipycnometer.

Glass samples for the HEXRD experiments were finely ground, and reacted in either SBF or TBS: 50 ml of SBF or TBS was heated to 37°C in a beaker and allowed to reach thermal equilibrium, after which 75 mg of the finely ground glass powder was added, with constant stirring, for times of 1, 2 and 10 h, 2, 6 and 7 days. After each time period, each solution was filtered, rinsed briefly with deionised water and then acetone. The reacted powders were then dried in an oven at 100°C overnight. The measured sample compositions after each reaction period are shown in Table 2.

Glass samples for the GIXRD experiments were prepared from glass discs roughly 20 mm in diameter and 4·5 mm thick. The samples were dry polished

Table 2. Sample compositions for TBS/SBF-reacted samples measured using x-ray fluorescence, using charge balancing to determine oxygen concentrations

	1 h	2 h	10 h	2 days	6 days	7 days
SBF samples						
at% (±0·003)						
Ca	0·100	0·106	0·083	0·119	0·088	0·130
Si	0·228	0·182	0·239	0·174	0·212	0·189
P	0·007	0·016	0·011	0·029	0·022	0·020
Na	0·017	0·024	0·009	0·003	0·004	0·004
O	0·648	0·672	0·652	0·675	0·674	0·657
TBS samples						
at% (±0·003)						
Ca	0·097	0·100	0·071	0·076	0·083	0·079
Si	0·228	0·208	0·241	0·237	0·229	0·235
P	0·009	0·019	0·016	0·017	0·017	0·016
Na	0·015	0·008	0·002	0·001	0·002	0·002
O	0·652	0·666	0·669	0·669	0·668	0·667

using polishing plates of 68, 36 and 12 μm, and then polished using diamond grit down to 0·5 μm to ensure an optically flat surface suitable for x-ray diffraction at shallow angles of incidence. For the reactions, 200 ml of the buffered model solution, TBS, was placed in a beaker and preheated to 37°C. The sample was placed, polished face up, in the beaker, covered with parafilm and placed back in the oven at 37°C to react for defined periods of time.

2.2. X-ray diffraction

The high energy x-ray diffraction (HEXRD) data was collected on Station 9.1 at the synchrotron radiation source (SRS), Daresbury Laboratory, UK. The finely powdered samples were enclosed inside a 0·5 mm thick circular metal annulus by kapton windows and mounted within a flat-plate instrumental set-up. The wavelength was set at λ=0·4875 Å, and calibrated using the K-edge of a Ag foil for the samples reacted with SBS; for the samples reacted in TBS, the wavelength was set at λ=0·5090 Å, and calibrated using the K-edge of a Pd foil. These values are low enough to provide data to a high value of wavevector transfer ($Q_{max}=4\pi\sin\theta_{max}/\lambda>20$ Å^{-1}). The data were corrected using a suite of programs written in-house, but based upon the methodology of Warren.[12,13]

The glancing angle XRD, GIXRD, data was collected using a Philips *X'Pert* diffractometer with a wavelength derived from the Cu K_α line (1·5405 Å). With the sample aligned correctly, the diffraction patterns obtained are biased towards the surface of the samples, although with some bulk scattering contributing an underlying diffraction pattern. As the depth of penetration of the x-rays is not known, and neither are the details of density and composition in the near surface regions, quantitative analysis of these results cannot be performed. However, a reliable interpretation of the growing crystalline phase on the surface can nevertheless be achieved.

Both XRD and analogous neutron diffraction methods are governed by the same generic physical principles. After data reduction and the consequent generation of the structure factor, $S(Q)$, from the experimentally determined interference function one may derive the associated real space pair correlation function, $T(r)$, by Fourier transformation via the following equation

$$T(r) = \frac{2}{\pi}\int_0^\infty QS(Q)\sin(Qr)\,\mathrm{d}r + T^0(r) \qquad (1)$$

where $T^0(r)$ is defined as

$$T^0(r) = 4\pi r\rho(\textstyle\sum_i n_i Z_i)^2 \qquad (2)$$

where ρ is the atomic number density; n_i is the fraction of atom type i, and Z_i is the corresponding atomic number (x-rays) or coherent scattering length (b_i) (neutrons). It is possible to obtain structural information from $T(r)$ (e.g. bond lengths, coordination numbers, etc.) via a modelling process. For multicomponent systems, such as under discussion here, $T(r)$ may also be defined in terms of the partial correlation functions, $T_{ij}(r)$, for pairs of atomic species i and j as

$$T(r) = \sum_{i,j} n_E n_j Z_i Z_j T_{ij}(r) \qquad (3)$$

Fitting Gaussians directly to $T(r)$ can be problematic for a multicomponent system due to the presence of overlapping pairwise correlations; this is exacerbated by truncation effects in the Fourier transformation process due to the finite range of the data (Q_{max} is ~22 Å^{-1} for the HEXRD data). Truncation effects can be ameliorated by the use of a window function, however this is at the expense of peak shape and width. These problems are partially overcome by simulating the $S(Q)$ with model peaks in $T(r)$. The simulated $S(Q)$ may be generated and transformed using the same Q range and window function as the experimentally-derived data, and may then be refined by iterating the parameters associated with the Gaussian model $T(r)$ correlations.[14] We note that the effective resolution of features within $T(r)$ is

$$\Delta r \sim \frac{2\pi}{Q_{max}} \qquad (4)$$

and for completeness, that the width of a given isolated peak in the S(Q) implies a coherence length in r-space of ~$2\pi/\Delta Q_{peak}$.

3. Results and discussion

The XRF analysis of composition presented in Tables 1 and 2 and Figures 2 and 3 reveals that the samples do not behave identically with respect to reaction in the two solutions (one a simulated physiological fluid, SBF, the other a standard cell culture medium, TBS), although both sets do nevertheless behave qualitatively as expected, with calcium, phosphorus

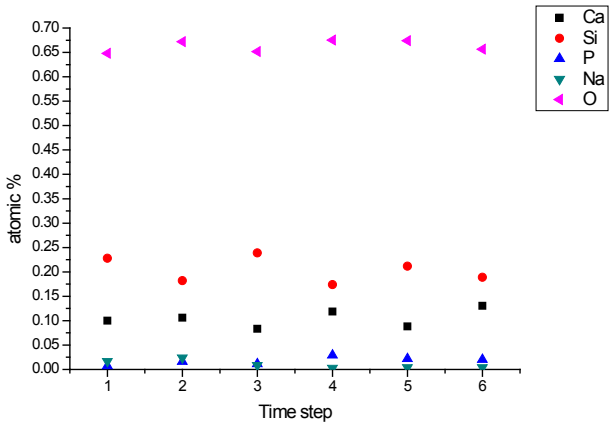

Figure 2. Graph to show the sample characterisation on the basis of XRF, (using charge balancing to determine oxygen concentrations), for samples reacted with SBF

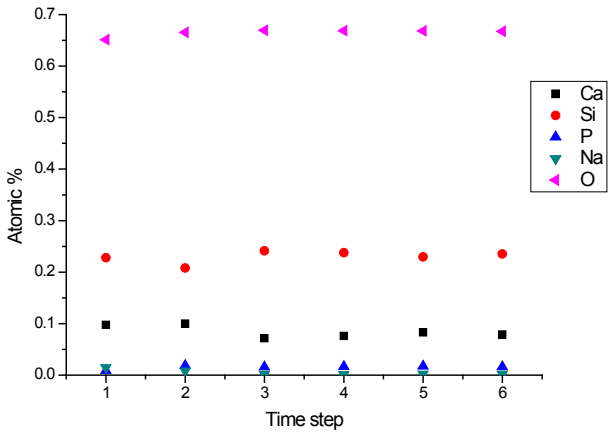

Figure 3. Graph to show the sample characterisation on the basis of XRF, (using charge balancing to determine oxygen concentrations), for samples reacted with TBS

and silicon content fluctuating as the reactions take place, and the sodium content decreasing as reaction time increases, reflecting an initial dissolution followed by a re-precipitation of calcium phosphate. It is the rates associated with these processes that vary between one set of samples and the other.

The structure of the unreacted material has been studied using HEXRD, MAS-NMR and reverse Monte Carlo modelling.[6] The ^{29}Si NMR suggested that the host silica network primarily consists of chains and rings of Q^2 SiO_4 tetrahedra, with some degree of cross linking as represented by the presence of Q^3 units. The ^{31}P NMR indicated that phosphorus exists as isolated PO_4^{3-} anions in the structure, which could tend to remove sodium and calcium cations from a network modifying role in the silicate network.

The diffraction data showed a broad Ca–O pair correlation at ~2·05–2·90 Å, with a total coordination of ~5 and suggested a Na–O distance of 2·38 Å and a corresponding coordination of ~6. This coordination number was supported by the ^{23}Na NMR data, which revealed that the likely sodium environment is six-coordinate in pseudo-octahedral NaO_6 arrangement, although there is the possibility of the presence of five-coordinate Na^+ ions.

There was evidence of a non-homogeneous distribution of Na within the glass, which is important in the context of the relatively slow dissolution of the modified silica network. The data also provided evidence of Ca clustering, and implied the presence of CaO as the structural motif. This latter observation was of direct relevance to the understanding of the facile nature of Ca within such glasses which gives rise to its relatively rapid diffusion from the solid into solution (and therefore to its behaviour in terms of the material's overall bioactivity).

3.1. HEXRD

Figures 4 and 5 show the high energy x-ray diffraction $S(Q)$'s and derived $T(r)$'s respectively for the samples of Bioglass reacted in SBF. Figures 6 and 7 show the corresponding high energy x-ray diffraction $S(Q)$'s and derived $T(r)$'s respectively for the samples reacted in TBS.

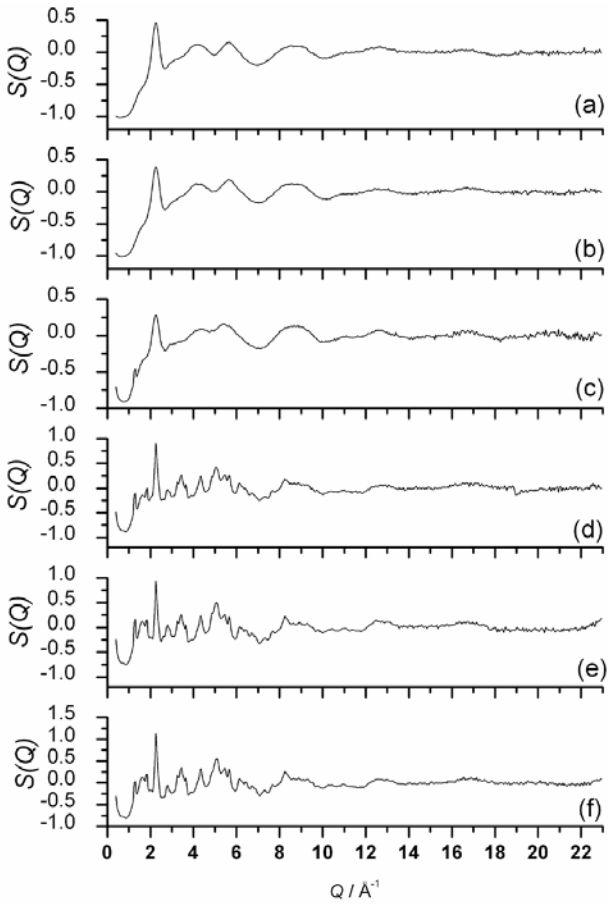

Figure 4. High energy x-ray diffraction Q-space data S(Q)*: (a) 1 h, (b) 2 h, (c) 10 h, (d) 2 days, (e) 6 days, (f) 7 days immersion time in SBF*

The data reveal subtle differences between the reaction in SBF compared to the reaction in TBS. In the $S(Q)$ data for both, the data shows that the sample begins amorphous (i.e. as a glass), and then as reaction time increases a calcium phosphate crystalline phase begins to appear. This can be seen after two days for the Bioglass sample immersed in SBF, however this stage occurs after only 10 h for the Bioglass sample immersed in TBS. As SBF contains P ions and TBS does not, one might expect that the growth of a calcium phosphate layer would occur faster for the Bioglass sample immersed in SBF, however the data seems to contradict this. It may be the case that the crystalline phase is observed earlier in the TBS solution because larger crystals are forming (albeit of lower total volume), which would make the observation of Bragg peaks in the HEXRD data significantly easier – that is to say, there may be a distinction to be drawn between the rate of crystal phase deposition and the time at which that phase is evident as well defined Bragg-like features. By seven days of immer-

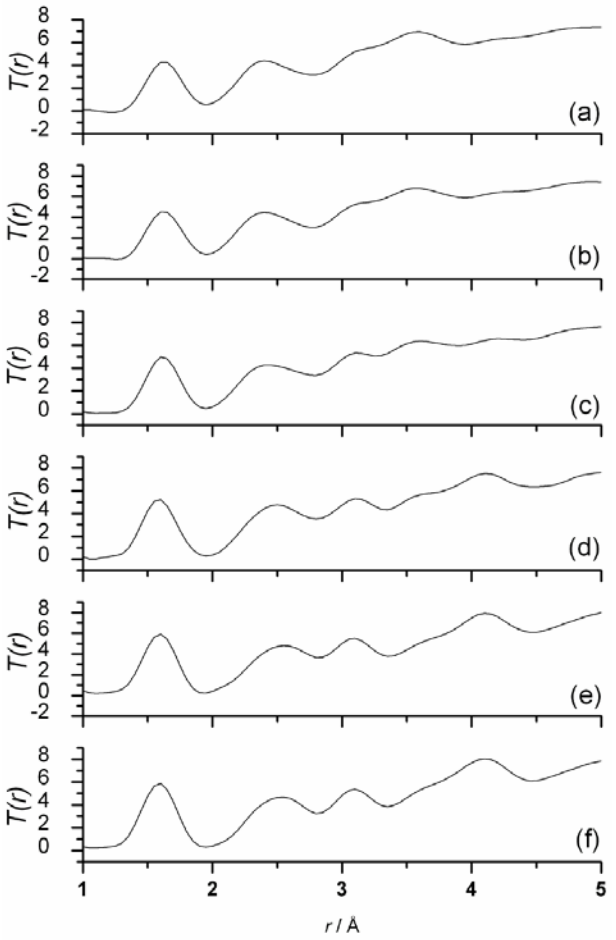

Figure 5. High energy x-ray diffraction r*-space data,* T(r)*: (a) 1 h, (b) 2 h, (c) 10 h, (d) 2 days, (e) 6 days, (f) 7 days immersion time in SBF*

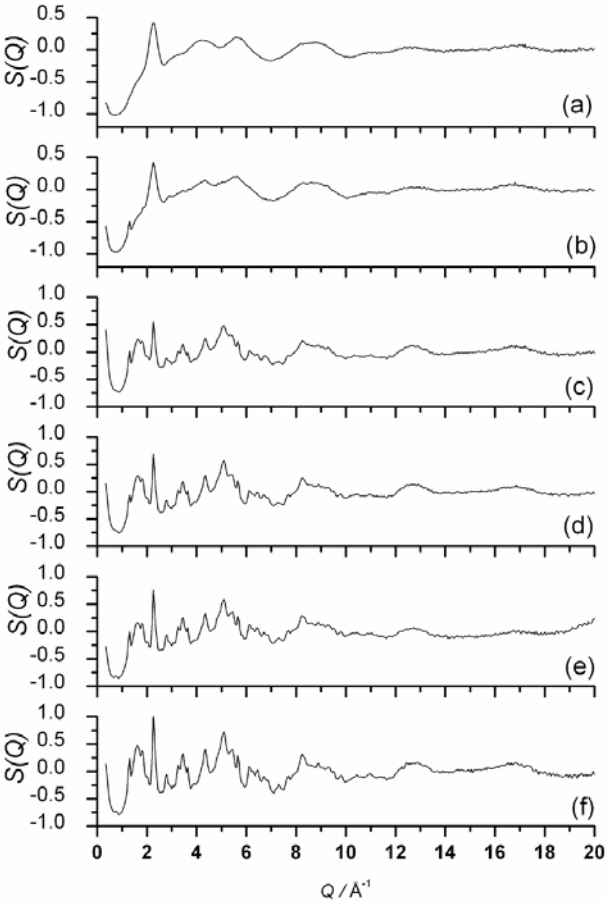

Figure 6. High energy x-ray diffraction Q*-space data,* S(Q)*: (a) 1 h, (b) 2 h, (c) 10 h, (d) 2 days, (e) 6 days, (f) 7 days immersion time in TBS*

sion time in each solution, the two samples appear to be at the same stage in the reaction process, with both samples showing very similar structure factors.

The main change observed in the *r-space* data is in the peak centred on ~3·1 Å, which corresponds to Si···Si, P···Ca, P···Si and Si···Ca pair correlation distances. In the TBS reacted sample this peak becomes becomes better defined after 10 h of reaction time, whereas in the SBF reaction the peak becomes more prominent after only two days reaction time. Also the peak centred on ~2·4 Å appears to shift to longer *r* (~2·6 Å) after the same reaction times. This may be due to the leaching of Na ions into the TBS/SBF, as is shown in the XRF data in Table 2: the peak at 2·4 Å, which may be assigned to the Na–O correlation, will decrease in area with respect to the other pairwise correlations at slightly longer distances. In the $T(r)$, as in the $S(Q)$, the samples appear to be at the same stage of the reaction process after seven days reaction time.

There are similarities between the data from the Bioglass samples and that obtained from calcia–silica sol-gel bioactive glass.[7] Most notably, the peaks at ~2·6 and ~3·1 Å also become more prominent as the reaction time increases. However, in terms of differences, one notes the absence of Na (and P) in the sol-gel samples which therefore posses an ostensibly simpler composition (although the presence of terminating hydroxyl groups in the sol-gel derived material must be considered). Furthermore, Skipper *et al* observed a peak in the *r-space* ND data at 2·02 Å which was assigned to second neighbour O···H correlations found in hydrated calcium phosphates, which is not visible in the data presented on the Bioglass samples reacted in either SBF or TBS.

3.2. GIXRD

Figure 8 shows the glancing incidence XRD data for the prepared glass sample before and after reaction with TBS at 37°C (for both 1 and 24 h). The data show that after 1 h, the relative amplitude of the diffuse scattering features has altered and thus structural changes are occurring in the vicinity of the glass surface, but the surface is evidently still amorphous. After 24 h in TBS however, significant structural changes are occurring on the surface and a crystalline phase is present. The data for the glass immersed in TBS for 24 h may be compared with diffraction data for hydroxyapatite,[15] as well as for forms of calcium phosphate that have previously

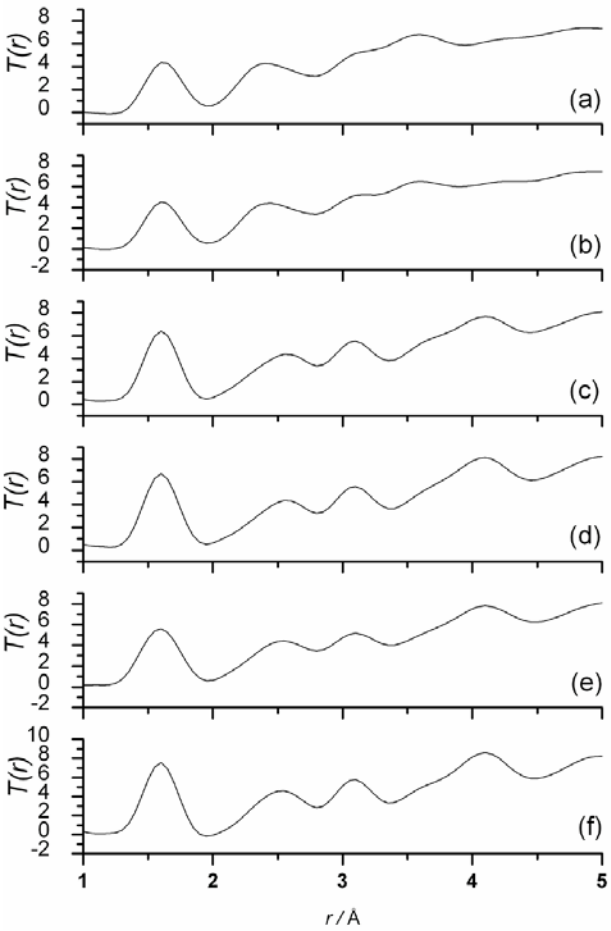

Figure 7. High energy x-ray diffraction r*-space data,* T(r)*: (a) 1 h, (b) 2 h, (c) 10 h, (d) 2 days, (e) 6 days, (f) 7 days immersion time in TBS*

been associated with the early stage mineralisation of the glass surface, namely tricalcium phosphate[16] and octacalcium phosphate.[17] Although the diffraction data for these three calcium phosphates is similar, the peak positions and intensities shown in Figure 9 are distinct enough to show that the crystalline phase on the surface of the Bioglass is hydroxyapatite. Furthermore, the variation in the relative strengths of

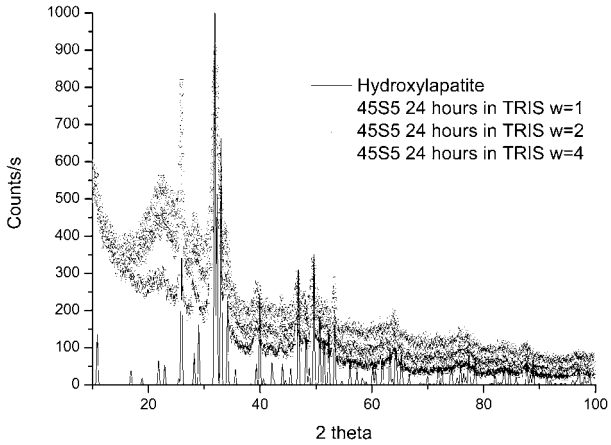

Figure 9. The variation in the GIXRD pattern for glass reacted for 24 h in TBS: ω=1, 2, 4°, and compared to diffraction data for hydroxyapatite (black line)

the amorphous (diffuse) scattering and the crystalline Bragg scattering with the angle of incidence (ω) shows clearly that the crystalline phase is surface related.

Thus, crystalline hydroxyapatite has formed on the surface of the glasses after 24 h immersion in TBS. These results agree with several sets of previously published data (using SBF, however, rather than TBS). For example, Kontonasaki *et al*[18] examined hydroxycarbonate apatite (HCA) formation on particulate Bioglass (Perioglass®) using Fourier transform infrared spectroscopy (FTIR) and scanning electron microscopy (SEM) with associated energy dispersive spectroscopy (EDS). They concluded that after 12 h in the SBF, an amorphous $CaO–P_2O_5$-rich layer had formed on the surface of the glass; after 24 h in SBF, a well defined crystalline HCA layer had formed on the surface. The results shown in the present study therefore indicate that one can expected a crystalline layer of hydroxyapatite to be formed on the surface irrespective of the details of the aqueous biomedical medium employed. Furthermore, although the data shown herein are not such that a definitive statement

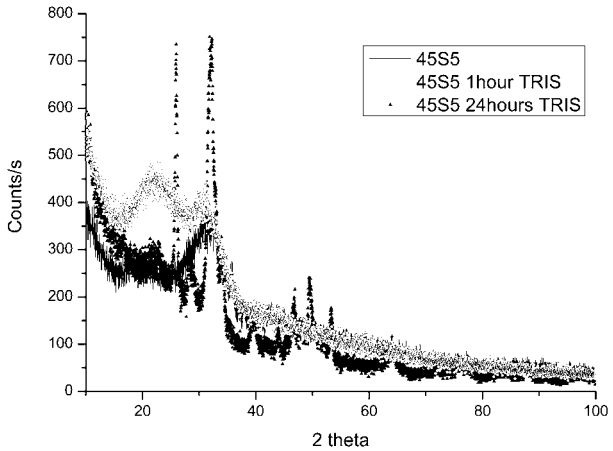

Figure 8. GIXRD data for Bioglass sample: unreacted, and after 1 and 24 h immersion in TBS; ω=1° for all samples

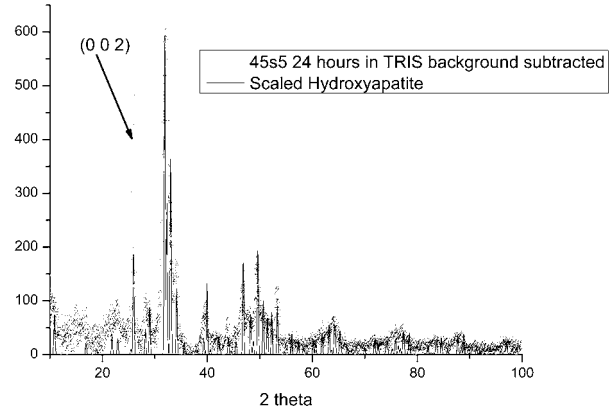

Figure 10. Comparison between the background corrected GIXRD pattern and hydroxyapatite showing the preferred orientation of hydroxyapatite grown after 24 h in TBS

may be made, the results suggest that the change in the amorphous surface may be associated with the beginnings of the growth of the amorphous $CaO–P_2O_5$ -rich layer observed by Kontonasaki *et al*.[18]

The GIXRD data show in addition that the hydroxyapatite layer may be growing with preferred orientation. Figure 10 shows the GIXRD data, after a low order polynomial has been used empirically to remove the underlying diffuse background, plotted against that from hydroxyapatite; the peak assigned to the (002) reflection is relatively strong compared to other peaks, indicating the hydroxyapatite layer may have a preferred orientation in the (001) plane. This phenomenon has been observed previously by Rehman *et al*[19] when observing the growth of apatite layers on Bioglass reacted in SBF for 7, 14 and 30 days, with the preferred orientation becoming less significant with time. The present data show that this occurs as early as 24 h immersion time in TBS.

Conclusions

High energy x-ray diffraction data show that after seven days immersion time the Bioglass in SBF appears to have the same overall structure as that immersed in TBS. The intermediate stages reveal that the Bioglass immersed in TBS generates well-defined Bragg diffraction peaks more rapidly than that in SBF, this may be due to the growth of larger crystals in the TBS case rather than a higher total crystallite volume.

The GIXRD data confirm the growth of hydroxyapatite on the surface of Bioglass when immersed in TBS. The data indicate that the hydroxyapatite crystals grow with a preferred orientation in the (001) plane.

Acknowledgements

The authors wish to thanks Dr Valentin Craciun (University of Florida) for his assistance in the collection of the GIXRD data. VF is grateful to the EPSRC for a studentship and to Novamin Inc. for funding her work in the USA.

References

1. Hench, L. L., Splinter, R. J., Allen, W. C. & Greenlee, T. K. *J Biomed Mater Res Symp*., 1971, **2** (Part I), 117–41.
2. Clark, A. E. & Hench, L. L *Biomed Mater Res*., 1976, **10**, 161–74.
3. See www.novabone.com and www.novamin.com for commercial details; *Bioglass*® is a registered trade mark.
4. Cerrutti, M., Bianchi, C. L., Bonino, F., Damin, A., Perardi, A. & Marterra, C. *J. Phys. Chem. B*, 2005, **109**, 14496–14505.
5. Tilocca, A., Cormack, A. N. & de Leeuw, N. H. *Chem. Mater.*, 2007, **19**, 95–103.
6. FitzGerald, V., Pickup, D., Greenspan, D., Sarkar, G., Fitzgerald, J., Wetherall, K. M., Moss, R. M., Jones, J. R. & Newport, R. J. A Neutron and X-ray diffraction study of Bioglass® with Reverse Monte Carlo modelling. *Adv. Func. Mater.*, 2007, **17**, 3746–3753.
7. Skipper, L. J., Sowrey, F. E., Pickup, D. M., Drake, K. O., Smith, M. E., Saravanapavan, P., Hench, L. L. & Newport, R. J. The structure of a bioactive calcia:silica sol-gel glass. *J. Mater. Chem.*, 2005, **15**, 2369–2374.
8. Newport, R. J., Skipper, L. J., Carta, D., Pickup, D. M., Sowrey, F. E., Smith, M. E., Saravanapavan, P. & Hench, L. L. The use of advanced diffraction methods in the study of the structure of a bioactive calcia:silica sol-gel glass. *J. Mater. Sci.-Mater. Med.*, 2006, **17**, 1003–1010.
9. FitzGerald, V., Drake, K. O., Jones, J. R., Smith, M. E., Honkimäki, V., Buslaps, T., Kretzschmer, M. & Newport, R. J *In-situ* High Energy X-ray Diffraction Study of a Bioactive Calcium Silicate Foam Immersed in Simulated Body Fluid. *J. Synchrotron Radiat.*, 2007, **14**, 492–499.
10. Kokubo, T., Kushitani, H. & Sakka, S. Solutions able to reproduce in vivo surface-structure changes in bioactive glass ceramic A-W. *J. Biomed. Mater. Res*., 1990, **24**, 721–734.
11. Hench, L. L. & Wilson, J. In: *Introduction to Bioceramics*, Eds: L. L. Hench & J. Wilson, World Scientific, Singapore, 1993, p 17.
12. Warren, B. E. *X-ray Diffraction*, Dover Publications, New York, 1990.
13. Cole, J. M., van Eck, E. R. H., Mountjoy, G., Anderson, R., Brennan, T., Bushnell-Wye, G., Newport, R. J. & Saunders, G. A. *J. Phys.: Condens. Matter*, 2001, **13**, 4105.
14. Gaskell, P. H. *Materials Science and Technology*, Vol. 9, Ed: J. Zrzycky, Weinhaim VCH, 1991, p 175.
15. de Andrade, A. V. C., da Silva, J. C. Z., Paiva-Santos, C. O., Weber, C., dos Santos Utuni, V. H., Tebcherani, S. M., Ferreira Borges, C. P., da Costa, E. & Martinez Manent, S. *Ceram. Eng. Sci. Proc*., 2004, **25,** 639–645.
16. Yashima, M., Sakai, A., Kamiyama, T. & Hoshikawa, A. *J. Solid State Chem*., 2003, **175**, 272–277.
17. Mathew, M., Brown, W. E., Schroeder, L. W. & Dickens, B. *J. Crystallogr. Spectrosc. Res*., 1998, **18**, 235–250.
18. Kontonasaki, E., Zorba, T., Papadopoulou, L., Pavlidou, E., Chatzistavrou, X., Paraskevopoulos, K. & Koidis, P. *Cryst. Res. Technol*., 2002, **37**, 1165–1171.
19. Rehman, I., Knowles, J. C. & Bonfield, W. *J. Biomed. Mater. Res.*, 1998, **41**, 162–166.